

Copyright 2005 Society of Photo-Optical Instrumentation Engineers.

This paper was published in the Proceedings, SPIE Symposium on Defense & Security, 28 March – 1 April, 2005 , Orlando, FL, Conference 5806 (Paper #17) and is made available as an electronic reprint with permission of SPIE. One print or electronic copy may be made for personal use only. Systematic or multiple reproduction, distribution to multiple locations via electronic or other means, duplication of any material in this paper for a fee or for commercial purposes, or modification of the content of the paper are prohibited.

Multi-resolution segmentation for improved hyperspectral mapping

F. A. Kruse
Horizon GeoImaging, LLC
4845 Pearl East Circle, Suite 101
Boulder, CO 80301-6113
Phone: 303-499-9471, Email: kruse@hgimaging.com
<http://www.hgimaging.com>

ABSTRACT

Many hyperspectral imagery (HSI) mapping methods currently attempt to determine the dimensionality of a dataset and extract discreet endmembers based on linear spectral mixing theory. The problem with this approach is that these datasets are often of such high dimensionality that it is difficult to extract the level of detail inherent in the data. Most such analysis approaches are simply overwhelmed by the complexity of HSI data. This research describes an approach that uses segmentation and iterative analysis of HSI data to reduce the dimensionality to a manageable level. The methodology involves spectral/spatial segmentation to determine initial groups of materials. The segmentation can be done using a variety of methods, including classical supervised or unsupervised classification methods, the Spectral Angle Mapper (SAM), spectral feature-based methods, or standard endmember determination and mapping approaches. The result of the segmentation is a broadly classified image. There may be significant variation within each class. These segments are then used as the starting point for additional n-Dimensional analysis. The HSI data are analyzed for each of the classes or segments using a linear mixing approach, endmembers are determined, and distributions and abundances are mapped. The segmentation reduces the original, complex dataset to a series of less complex problems. Combination of the segment results to a composite analysis result produces a materials map that includes additional detail beyond that achieved using the whole-image approaches. A case history utilizing AVIRIS data is presented.

KEYWORDS: HSI Segmentation, Hyperspectral Analysis, Multiresolution Analysis

1. INTRODUCTION

Hyperspectral Imagery (HSI data) are noted for their high dimensionality compared to multispectral imagery (MSI) data^{1,2}. Hyperspectral data, with many (often hundreds) of spectral bands, allow extraction of diagnostic spectral features that make identification of unique materials (endmembers) possible³. Many researchers have used an n-dimensional analysis approach to determine key endmembers and map their distribution and abundances⁴. This approach works well for geologic and other similar problems, but high data dimensionality often limits its utility for complex scenes such as those typical of urban areas and other complex, highly variable environments⁵.

Use of segmentation prior to analysis allows breaking the complex problem into a number of smaller (lower dimension) analyses. Airborne Visible/Infrared Imaging Spectrometer (AVIRIS) data⁶ acquired of Boulder, Colorado during October 2002 on NASA's ER-2 aircraft at approximately 15m spatial resolution⁵ are used here to demonstrate segmentation concepts and their application.

2. METHODS

Two different segmentation approaches were applied to the AVIRIS data; 1) Spectral segmentation using the Spectral Angle Mapper (SAM), and 2) Spatial/Spectral segmentation using the eCognition software. A modified, automated hourglass procedure consisting of MNF transform, PPI, clustering of thresholded PPI data for endmember extraction, and Spectral angle Mapper (SAM) as a 1st cut classification was applied to both segmentation results. In this approach, hyperspectral data are used to determine spectral endmembers at the subpixel level using standardized HSI subpixel mapping techniques^{3,7} (Figure 1). Iteration is used on segmented data to reduce the dimensionality of the problem to manageable pieces.

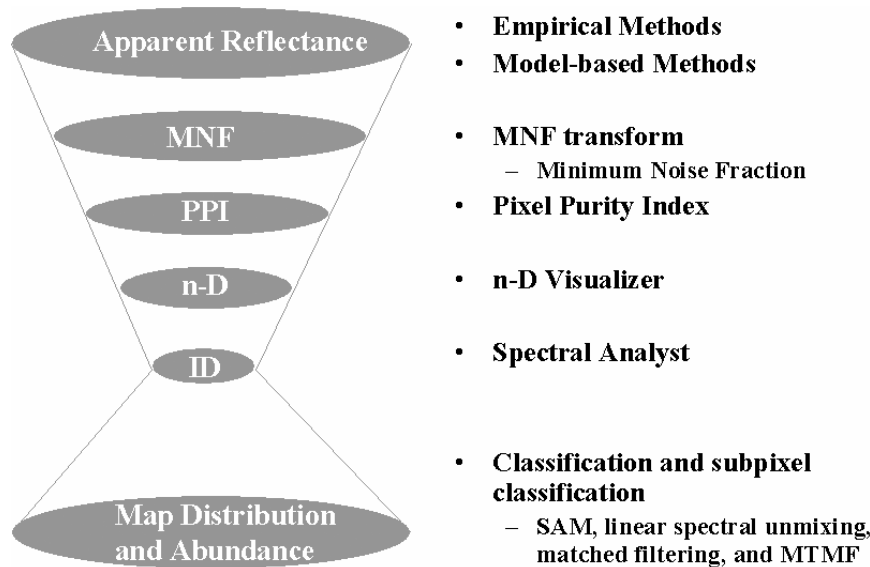


Figure 1: Standardized hyperspectral analysis scheme. Note the hourglass shape, which schematically represents the reduction of the hyperspectral data to just a few key spectra at the neck and then expansion back to spectral maps of the full dataset. This approach is used iteratively on the segmentation results.

These methods were developed by Analytical Imaging and Geophysics, LLC (AIG) while the author was associated with that company. They also are implemented and documented within the Environment for Visualizing Images (ENVI) software system originally developed by AIG scientists (now a Research Systems Inc [RSI] commercial-off-the-shelf [COTS] product)⁸. They are also described briefly below. This is not the only way to analyze these data, but we have found that it provides a consistent way to extract spectral information from hyperspectral data without a priori knowledge or requiring ground observations. The analysis approach consists of the following steps:

1. correction for atmospheric effects using an atmospheric model ACORN⁹.
2. spectral compression, noise suppression, and dimensionality reduction using the Minimum Noise Fraction (MNF) transformation^{8, 10, 11}.
3. determination of endmembers using geometric methods (Pixel Purity Index – PPI)^{8, 11}.
4. extraction of endmember spectra using n-dimensional scatter plotting^{8, 11}.
5. identification of endmember spectra using visual inspection, automated identification, and spectral library comparisons¹².
6. production of endmember maps using a variety of mapping methods. The Spectral Angle Mapper (SAM) algorithm¹³ is used as a first-cut mapping method. The preferred mapping method Mixture-Tuned-Matched-Filtering (MTMF) provides more precise results and is basically a partial linear spectral unmixing procedure, producing abundance information for each endmember¹⁴.

2.1 Spatial/Spectral Segmentation and Analysis using SAM:

The procedure tested for the spectral (SAM) segmentation consisted of:

1. Standard hourglass analysis of the VNIR AVIRIS data to produce a SAM classification image
2. Extraction of segmentation masks (one for each SAM class)
3. For each spectral segment (SAM Class)
 - a. Localized MNF transform and automatic noise cutoff
 - b. Local PPI and automatic thresholding
 - c. Automated n-D scatterplotting, using clustering to extract potential endmembers
 - d. Spectral Angle Mapper and/or Mixture-Tuned-Matched-Filtering to individually map each segment
 - e. Interactive review and analysis

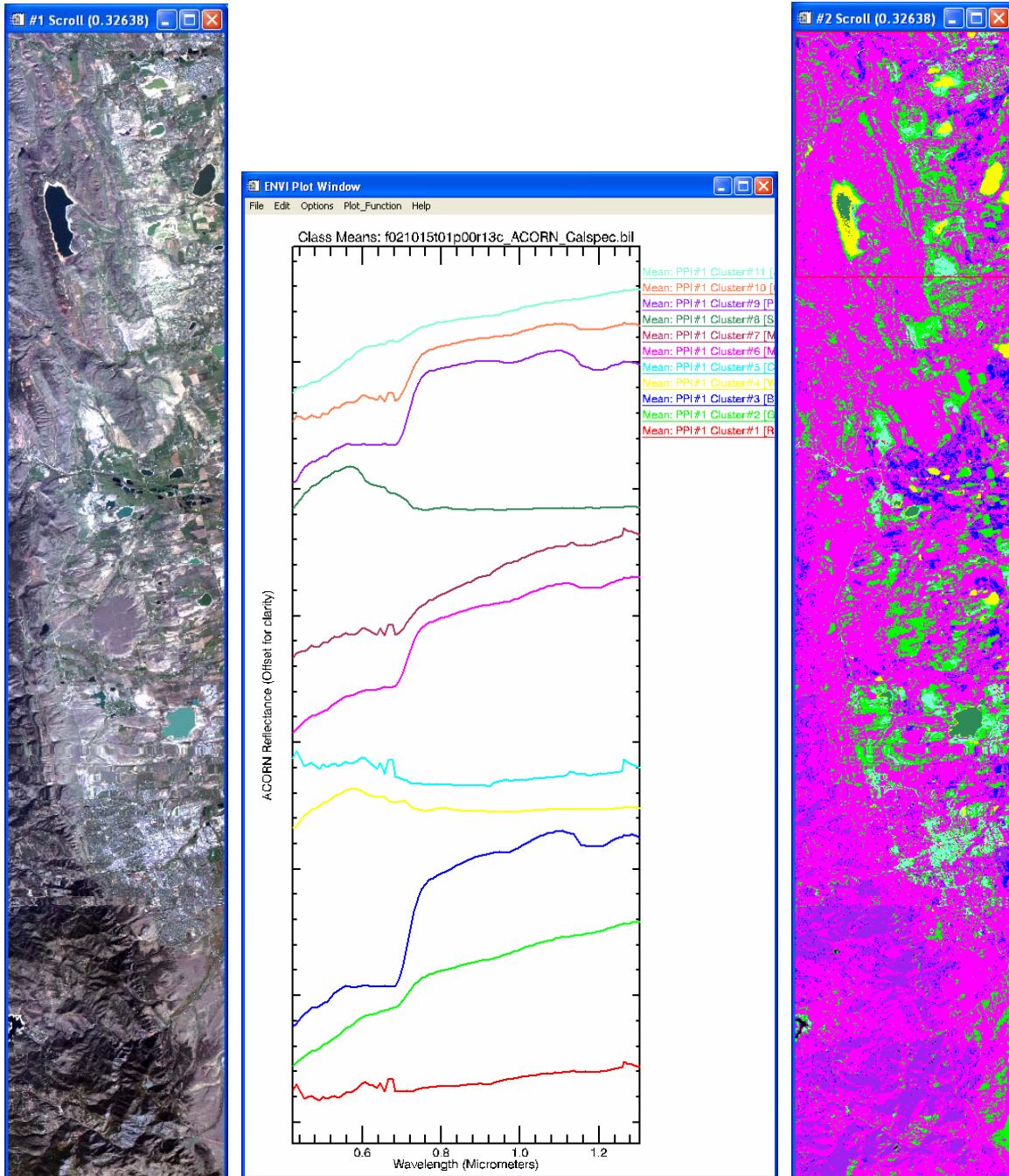


Figure 1: Left: True Color AVIRIS Image. Center: spectral endmembers extracted from the data using the standard (full-image) hourglass method. Right: Automated 1st-pass SAM classification of AVIRIS VNIR (0.4 - 1.3 μ m). Eleven SAM classes (+unclassified) found during the first automated analysis were used as segments for further analysis. Figures 2 and 3 and Table 1 show further segment analysis details.

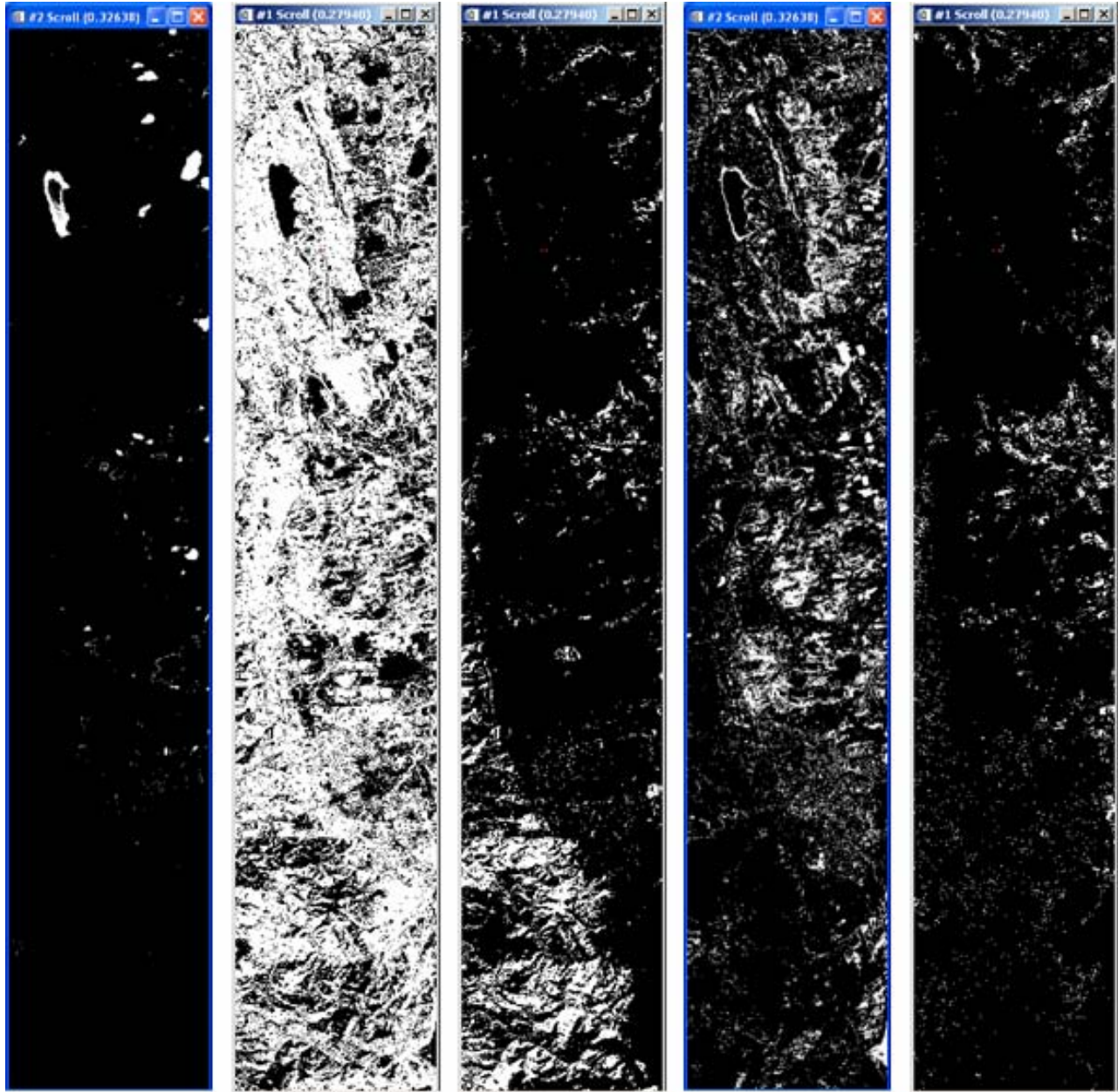


Figure 2: Five different (selected) SAM classes shown as binary mask images. The masks were used to generate localized MNF transformations. PPI was run on the masked MNF data using an automated data/noise cutoff. New endmembers were determined for each masked segment for use in the next stage of analysis.

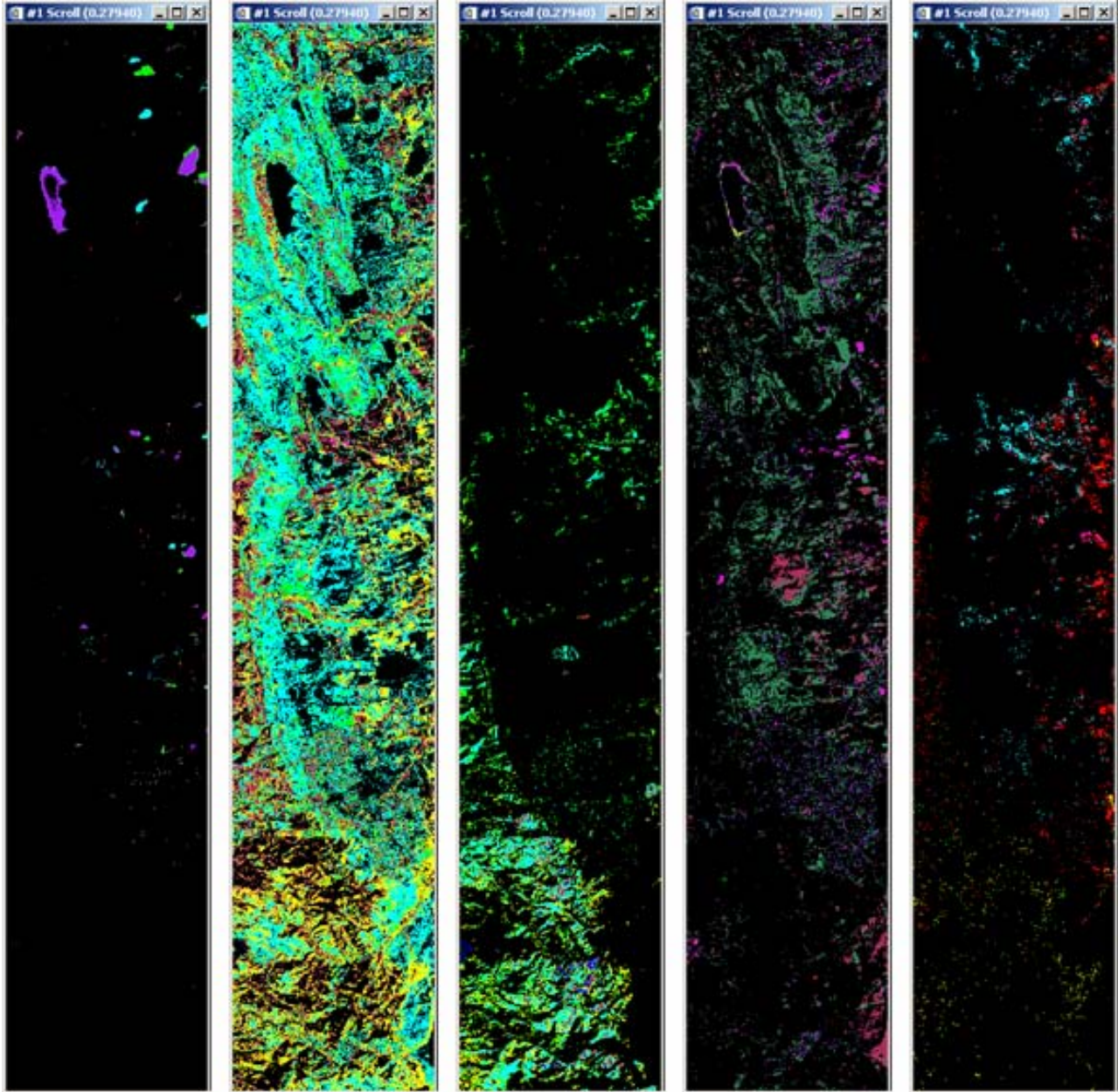


Figure 3: Second SAM classification of segmented images. Classifications are based on use of local segment endmembers determined from the MNF, PPI, automatic endmember clustering described above. Note additional detail in selected classes compared to Figure 2. Table 1 show number of classes in each segment and Figure 4 shows endmembers extracted for fourth image from left (SAM Segment 3).

SAM Segment*	# Classes
0 (unclassified)**	4
1	14
2	9
3	7
4	12
5	14
6	7
7	17
8	5
9	5
10	12
11	10
Total Classes	116

Table 1: Breakdown of new classes for each original SAM segment.

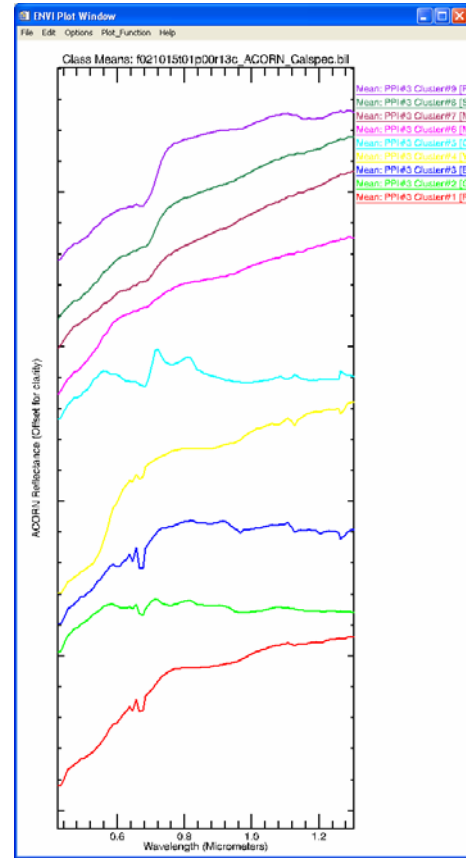


Figure 4: Endmembers extracted for segment 3 only (fourth Image from the left in Figure 3). These were previously all included in average for endmember #2 (Green) in Figure 3.

2.2 Spatial/Spectral Segmentation and Analysis using eCognition

An alternative segmentation was run using the eCognition spatial/spectral analysis software. eCognition specializes in multiresolution segmentation using an object-oriented approach. Multiresolution segmentation separates adjacent regions in an image as long as they have sufficient contrast based on certain spatial/spectral homogeneity measures. Multi-resolution segmentation with the eCognition software was used to produce spatial segments for more detailed spatial/spectral analysis. eCognition's multi-resolution segmentation uses region-merging starting with 1-pixel objects. Smaller objects are iteratively merged into larger ones using a pair-wise region growing process. This approach minimizes average heterogeneity of image objects weighted by their size (pairs of adjacent objects are merged that result in the smallest growth in heterogeneity¹⁵). The procedure tested consisted of:

1. Perform multi-resolution segmentation using eCognition on the VNIR MNF data
2. Convert segmentation results to ENVI Classification
3. Extract Segmentation Masks from classification image
4. For each spatial segment
 - a. Localized MNF transform and automatic noise cutoff
 - b. Local PPI and automatic thresholding
 - c. Automated n-D scatterplotting, using clustering to extract potential endmembers
 - d. Spectral Angle Mapper and/or Mixture-Tuned-Matched-Filtering to individually map each segment
 - e. Interactive review and analysis



Figure 5: Left: True Color AVIRIS Image. Right: eCognition 10-segment image. Figures 6 and 7 and Table 2 show further segment analysis details.

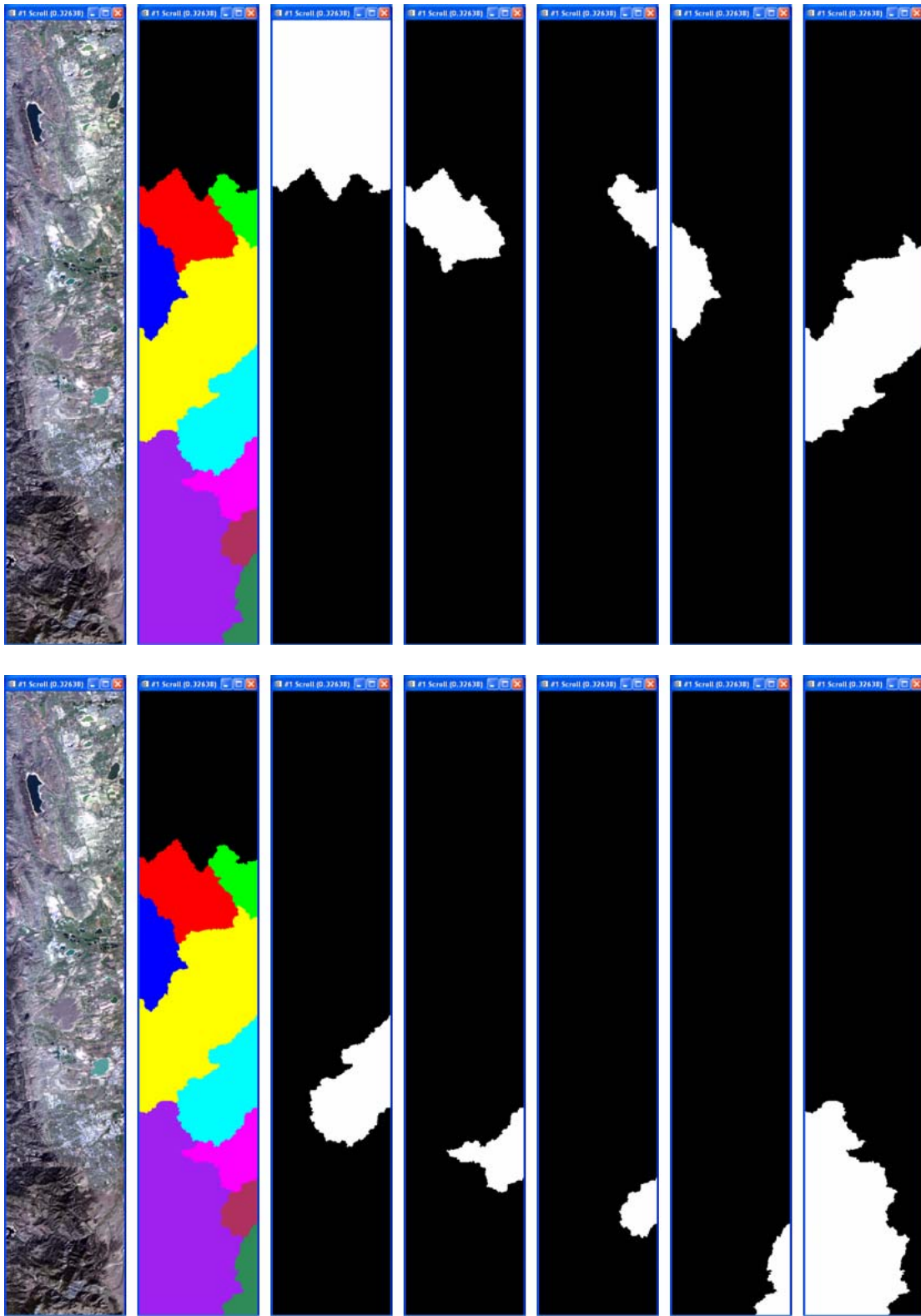


Figure 6: Left: True Color AVIRIS Image. 2nd from Left: eCognition segmentation results as ENVI classification image. Images starting 3rd from left are eCognition segmentation images as binary mask images. Note spatially distinct segments based on spectral homogeneity.

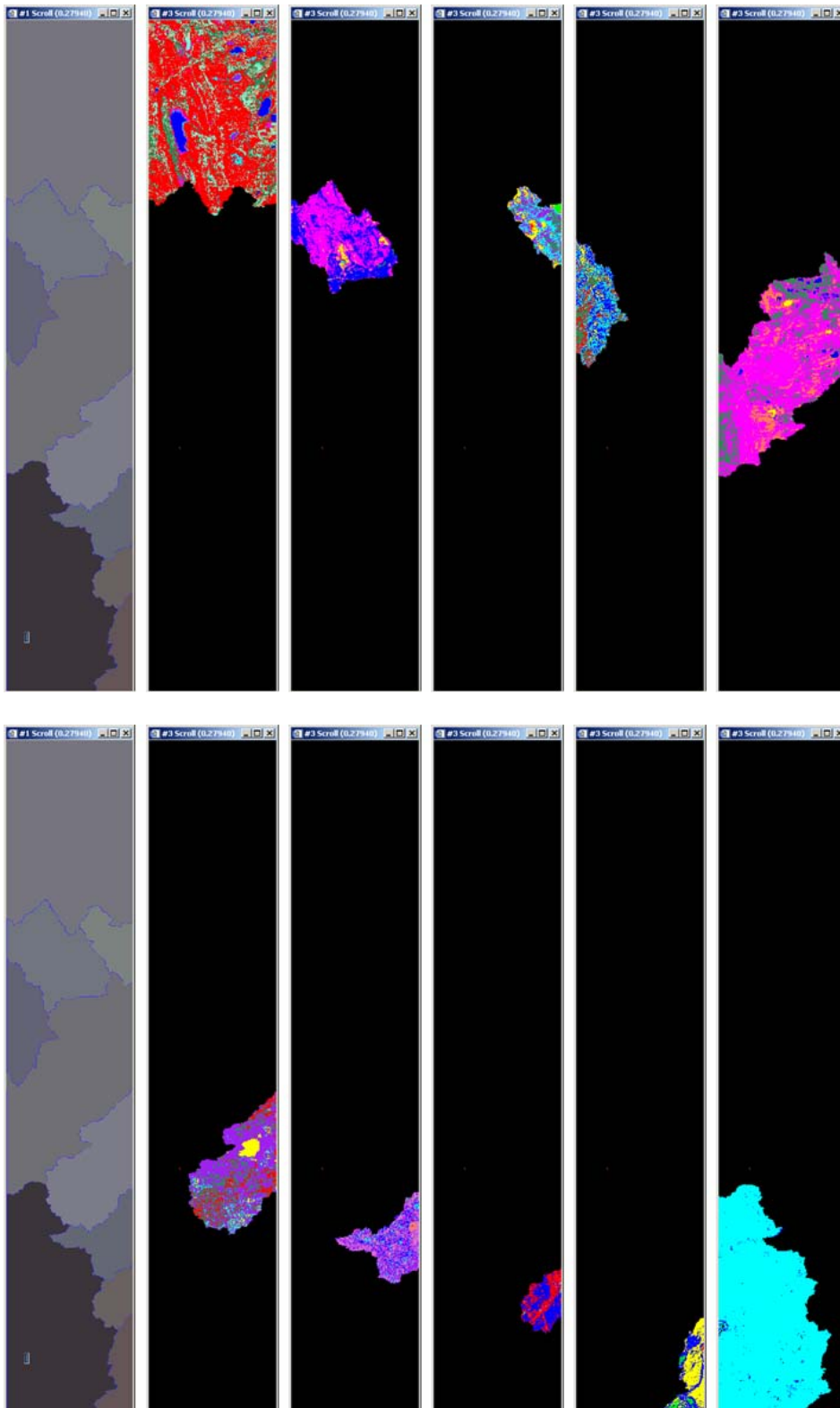


Figure 7: Left: eCognition segmentation result image. Images starting 2nd from left are result of applying localized segment MNF, PPI, automated endmember extraction, and SAM mapping to the individual segments. Note additional detail compared to Figure 1. Table 2 shows number of classes in each segment.

Segment ID	# EM
Segment 1	11
Segment 2	9
Segment 3	9
Segment 4	8
Segment 5	10
Segment 6	9
Segment 7	12
Segment 8	6
Segment 9	4
Segment 10	6
Total EM	84

Table 2: Breakdown of new classes for each original SAM segment.

3. DISCUSSION AND CONCLUSIONS

The above two segmented analyses examples illustrate the general concept of breaking the HSI analysis down into smaller problems and a preliminary methodology. The segmentation can be done using a variety of methods, including classical supervised or unsupervised classification methods; the Spectral Angle Mapper (SAM), spectral feature-based methods, or standard endmember determination and mapping approaches. The starting point of the segmentation is a broadly classified image and further within-segment classification makes the most sense when there is significant variation within each original class. Independent analysis of each segment reduces the original, complex dataset to a series of less complex problems. Combination of the segment results to a composite analysis result produces a materials map that includes additional detail beyond that achieved using the whole-image approaches. The research presented here, however, represents only the first stage. Additional work is still needed to validate segmentation results in terms of real-world spatial/spectral associations and to develop methods to compare endmembers from the various segments and consolidate, merge, and identify.

4. ACKNOWLEDGEMENTS

AVIRIS data were provided by Jet Propulsion Laboratory and research was supported by JPL Contract 1260713.

5. REFERENCES CITED

1. Goetz, A. F. H., G. Vane, J. E. Solomon, and B. N. Rock, 1985. Imaging spectrometry for earth remote sensing, *Science*, 228, 1147 - 1153.
2. Kruse, F. A., 1999, Visible/Infrared Sensors and Case Studies, Chapter 11, in Rencz, A., (ed.), *Remote Sensing for the Earth Sciences, Manual of Remote Sensing, Volume 3*, p. 567 - 606.
3. Kruse, F. A., Boardman, J. W., and Huntington, J. F., 2003, Evaluation and Validation of EO-1 Hyperion for Mineral Mapping: in Special Issue, *Transactions on Geoscience and Remote Sensing (TGARS)*, IEEE, v. 41, no. 6, June 2003, p. 1388 - 1400.
4. Boardman, J. W., 1993, Automated spectral unmixing of AVIRIS data using convex geometry concepts: in *Summaries, Fourth JPL Airborne Geoscience Workshop, JPL Publication 93-26*, 1: 11 - 14.
5. Kruse, F. A., Boardman, J. W., and Livo, K. E., 2004, Using Hyperspectral Data for Urban Baseline Studies, Boulder, Colorado: In proceedings 13th JPL Airborne Geoscience Workshop, Jet Propulsion Laboratory, 31 March - 2 April 2004, Pasadena, CA (in press).
6. Green, R. O., M. L. Eastwood, and C. M. Sarture, *Imaging Spectroscopy and the Airborne Visible Infrared Imaging Spectrometer (AVIRIS)*, *Remote Sens Environ* 65: (3) 227-248 SEP 1998.

7. Boardman, J. W., and Kruse, F. A., Automated spectral analysis: A geological example using AVIRIS data, northern Grapevine Mountains, Nevada: in Proceedings, Tenth Thematic Conference, Geologic Remote Sensing, 9-12 May 1994, San Antonio, Texas, p. I-407 - I-418, 1994.
8. Research Systems Inc(RSI), ENVI User's Guide, Research Systems Inc, 1084 p., 2003.
9. Analytical Imaging and Geophysics LLC (AIG), ACORN User's Guide, Stand Alone Version: Analytical Imaging and Geophysics LLC, 64 pp, 2001.
10. Green, A. A., Berman, M., Switzer, B., and Craig, M. D., A transformation for ordering multispectral data in terms of image quality with implications for noise removal, IEEE Transactions on Geoscience and Remote Sensing, v. 26, no. 1, p. 65 - 74, 1988.
11. Boardman, J. W., Kruse, F. A., and Green, R. O., Mapping target signatures via partial unmixing of AVIRIS data: in Summaries, Fifth JPL Airborne Earth Science Workshop, JPL Publication 95-1, 1: 23-26, 1995.
12. Kruse, F. A., Lefkoff, A. B., and Dietz, J. B., Expert System-Based Mineral Mapping in northern Death Valley, California/Nevada using the Airborne Visible/Infrared Imaging Spectrometer (AVIRIS): Remote Sensing of Environment, Special issue on AVIRIS, May-June 1993, v. 44, p. 309 - 336, 1993.
13. Kruse, F. A., Lefkoff, A. B., Boardman, J. B., Heidebrecht, K. B., Shapiro, A. T., Barloon, P. J., and Goetz, A. F. H., The Spectral Image Processing System (SIPS) - Interactive Visualization and Analysis of Imaging Spectrometer Data: Remote Sensing of Environment, Special issue on AVIRIS, May-June 1993, v. 44, p. 145 - 163, 1993.
14. Boardman, J. W., Leveraging the high dimensionality of AVIRIS data for improved subpixel target unmixing and rejection of false positives: mixture tuned matched filtering, in Summaries of the Seventh Annual JPL Airborne Geoscience Workshop, Pasadena, CA, 55 pp, 1998.
15. Definiens Imaging, 2004, eCognition Users Guide 4 (On-Line Documentation)